Study of Natural Convection in a Horizontal Square Enclosure with 4-Inner Heated Rods

Muneer A. Ismael
Mechanical Engineering Department
College of Engineering
Basra University
muneerismael@yahoo.com

Falah A. Abood
Mechanical Engineering Department
College of Engineering
Basra University

Sana J. Yaseen
Mechanical Engineering Department
College of Engineering
Basra University

Abstract

Laminar, natural convection heat transfer of air filling horizontal space between isothermal (cold) square enclosure and four isothermal (hot) cylindrical rods has been theoretically studied. Finite element method has been used to solve the conservation of governing equations by using software package (FlexPDE).

Parametric study has been conducted for the range of Rayliegh number$10^3 \leq Ra \leq 10^5$, Aspect ratio $0.11 \leq AR \leq 0.28$. Results are presented in the form of streamlines, isotherms contours and Nusselt numbers. Results showed that the overall heat transfer increases with increasing of both Ra and AR. The values of mean Nusselt numbers are compared with data reported in Ref. [6] and [15], and good agreement has been achieved.

Keywords: Natural convection, square enclosure, penalty.

دراسة نظرية للحمل الحر داخل فجوة افقية مسخنة بأربعة قضبان أسطوانية

المستخلص

تم في هذا البحث دراسة نظرية لأنتقال الحرارة بالحمل الحر الطباقي لهواء داخل فجوة أفقية بين أربعة قضبان اسطوانية مسخنة بدرجة حرارة ثابتة موضوعة داخل وعاء مربع الشكل معرض لدرجة حرارة ثابتة (بارد). أستخدمت طريقة العناصر المحددة بمساعدة الحقيبة البرمجية (Flex PDE) لحل معادلات الحفظ الحاكمة. كانت قيم المتغيرات لرقم رايلي تتراوح بين 10^3 الى 10^5 وقيم النسبة الثابتة من قطر الانبوب الى طول ضلع المربع Aspect ratio D/L تتراوح بين،0.11 الى 0.28. مُثلت النتائج بواسطة خطوط الجريان والتحارر ورقم نسلت حيث أظهرت النتائج تحسن انتقال الحرارة مع زيادة كل من Ra و AR . قورنت النتائج لمعدل رقم نسلت مع النتائج المنشورة في [6] و [15] واظهرت توافقاً جيد.

1. Introduction

The flow and thermal fields in enclosed space are of great importance due to their wide applications such as in solar collector-receivers, insulation and flooding protection for buried pipes used for district heating and cooling, cooling systems in nuclear reactors, etc. Large numbers of researches were published in the past few decades. Concentric and eccentric cases in a horizontal annulus between two circular cylinders have been well studied. The extensive research studies using various numerical simulations reported by [1-5] ensure that several attempts have been made to acquire a basic understanding of natural convection flows and heat transfer characteristics in an enclosure. Shu et al [6] studied numerically the natural convection in an eccentric annulus between a square outer cylinder and a circular inner cylinder using Different Quadrate (DQ) method, a symmetric study is conducted for the analysis and thermal fields at different eccentricities and angular positions. Shi and Khodadi [7] indicated that a partition attached to the heated vertical wall of square cavity degraded the heat transfer capacity on the wall of the cavity. The work of [8] also considered the natural convection in a square cavity with special side-wall temperature variation. Wu and Ching [9] investigated experimentally a square cavities with a temperature difference a cross the top and bottom walls. They found the flow pattern in the partitioned cavity was dependent on the top wall temperature of the cavity, the partition height and partition location. Mobedi [10] used the heat line technique to observe heat transport in the entire domain of a square cavity with thick horizontal walls. Recently, the heat line and streamline formulations were employed by [11] to demonstrate the heat flow for differentially and distributed heating walls with cavities. Wu and Ching [12] studies were on partitioned cavities with temperature difference in both horizontal and vertical directions, although results from cavities with smooth walls suggest of a partitioned square cavity. However, in the present research, the effect of four inner rods aspect ratio on natural convection heat transfer is to be studied for different Rayliegh numbers. The tool of investigation is finite element method implicated in a Flex PDE software package.

2. Governing equations

A schematic view of a horizontal space between a square enclosure and 4-inner cylindrical rods is shown in Fig.1. Heat is generated uniformly in the circular inner rods. Thermo physical properties of the fluid in the flow model assumed to be constant except the density variations causing a body force term in the momentum equation. The Boussinesq approximation is invoked for the fluid properties to relate density changes, and to couple in

this way the temperature field to the flow field. The governing equations for the steady natural convection flow using conservation of mass, momentum and energy can be written in the dimensionless form as:

$$\frac{\partial U}{\partial X}+\frac{\partial V}{\partial Y}=0 \tag{1}$$

$$U\frac{\partial U}{\partial X}+V\frac{\partial U}{\partial Y}=-\frac{\partial P}{\partial X}+\frac{\partial^2 U}{\partial X^2}+\frac{\partial^2 U}{\partial Y^2} \tag{2}$$

$$U\frac{\partial V}{\partial X}+V\frac{\partial V}{\partial Y}=-\frac{\partial P}{\partial Y}+\frac{\partial^2 V}{\partial X^2}+\frac{\partial^2 V}{\partial Y^2}+\left(\frac{Ra}{\Pr}\right)\theta \tag{3}$$

$$U\frac{\partial \theta}{\partial X}+V\frac{\partial \theta}{\partial Y}=\frac{1}{\Pr}\left(\frac{\partial^2 \theta}{\partial X^2}+\frac{\partial^2 \theta}{\partial Y^2}\right) \tag{4}$$

Non-dimensional parameters can be given as follows

$X=\frac{x}{L}$, $Y=\frac{y}{L}$, $U=\frac{uL}{\upsilon}$, $V=\frac{vL}{\upsilon}$, $\theta=\frac{T-T_o}{T_i-T_o}$, $P=\frac{(p+\rho gy)L^2}{\rho v^2}$, Prandtl number

$\Pr=\frac{\upsilon}{\alpha}$ and Rayleigh number $Ra=\frac{g\beta(T_i-T_o)L^3}{\upsilon\alpha}$

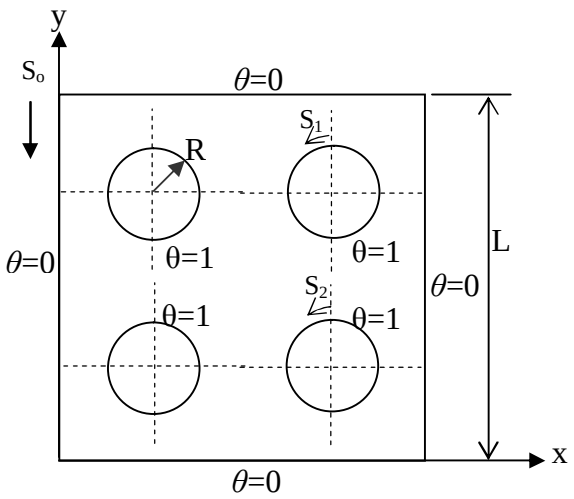

Figure (1). Schematic diagram of the physical domain.

The following Boundary conditions are used:

1- Isothermal surfaces i.e. θ=1 on the inner rods walls and θ=0 on the outer square walls.

2- No-slip velocity boundary condition, U=V=0 on all solid walls.

3- Pressure gradient normal to all surfaces is zero, $\frac{\partial P}{\partial n} = 0$ where n is normal unit vector.

Here X and Y are dimensionless coordinates varying along horizontal and vertical directions respectively; U and V are dimensionless velocity components in the X and Y directions, respectively. θ is the dimensionless temperature; P is dimensionless pressure.

3. Numerical solution

The momentum and energy balance equations are solved using finite element software Package (FlexPDE) [13]. The continuity Equation (1) is to be used as a constraint due to mass conservation and this constraint may be used to obtain the pressure distribution [14]. In order to solve Equations.(2)-(4), we use a penalty parameter and the incompressibility criterion by Equation.(1) which results in:

$$\nabla^2 P = \lambda\left(\frac{\partial U}{\partial X} + \frac{\partial V}{\partial Y}\right) \tag{5}$$

λ is a penalty parameter that should be chosen either from physical knowledge or by other means[12]. A most convenient value for λ was attained in this study to be (10^{11} *μ/L^2). The numerical solutions are obtained in terms of velocity components (U,V) and the stream function (ψ) is evaluated using the relationship between the stream function (ψ) and velocity components (U,V) as:

$$\frac{\partial^2 \Psi}{\partial X^2} + \frac{\partial^2 \Psi}{\partial Y^2} = \frac{\partial U}{\partial Y} - \frac{\partial V}{\partial X} \tag{6}$$

It may be noted that the positive sign of ψ denotes anti-clockwise circulation and the clock wise circulation is represented by the negative sign of ψ.

The no-slip condition is valid at all solid boundaries as there is no cross-flow, hence ψ=0 is used for the solid boundaries.

The heat transfer coefficient in terms of the local Nusselt number Nu_L along the inner rod surface and the outer wall is defined by:

$$Nu_L = -\frac{\partial \theta}{\partial n} \tag{7}$$

Where n is the normal direction on a plane. At steady- state it is obvious that the mean Nusselt numbers along both the inner and outer walls are exactly identical. Hence, the average Nusselt number can be evaluated along the outer wall only as:

$$Nu_m = \frac{1}{S_o}\int_{So} Nu_L ds_o \qquad (8)$$

4. Validations

4.1 Software validation

To check the validation of the software, the grid dependency and the continuity equation in addition are checked. The obtained results showed an exactly validation of the velocity distribution for a grid size obtained by imposing an accuracy of 10^{-4}. This accuracy is a compromised value between the results accuracy and the time consumed in each run. The girded domain for the enclosure of AR=0.23 is shown in Figure (2a) and the distribution of the values of ($\partial U/\partial X + \partial V/\partial Y$) over the domain, is presented in Figure (2b).

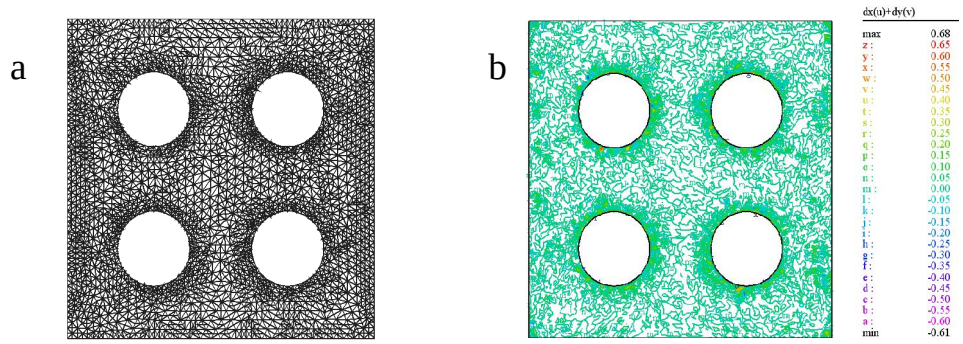

Figure (2). (a) Grid distribution over the domain (b) Validation of continuity equation, for 10^{-4} accuracy.

4.2 Validation of numerical results

In order to validate the employed numerical method more and more, results are obtained and compared with some reported data and found in good agreement. In the work of [6] work of [15], a single circular inner heated rod was concentrically located inside a square enclosure. The average Nusselt number Nu_m along the outer wall between the present work and the work of [6] is compared for $Ra=10^4$, $Pr=0.71$ for different values of (RR = L/2R) equal to 1.67 , 2.5 and 5 as shown in Table (1) . From this table, it can be seen that the present results generally agree well with that reported in [15] and very well with [6].

Table (1). Comparison of Nu_m between the present work and the works of [6] and [15] for $Ra=10^4$

L/D	Nu_m (present)	Nu_m [6]	Nu_m [15]
1.67	5.386	5.395	5.82
2.5	3.282	3.245	3.331
5	2.229	2.082	2.071

5. Results and discussion

5.1 Analyses of flow and thermal fields

To evaluate the aim of the present study, the streamlines, isothermal lines, and local and average Nusselt numbers were visualized and examined for different cases composed of different Rayliegh numbers ($Ra=10^3$-10^5) and different aspect ratios (AR= 0.11, 0.16, 0.23, 0.28).

The streamlines inside the enclosure of AR=0.23 are presented in the left side of Figure (3) for three values of Ra. At $Ra=10^3$, Figure (3a) , six circulation cells are formed inside the enclosure. Four of them are localized in each space between each rod and enclosure corner. The other two circulation cells are more strength and localized near the mid span of each vertical wall. The mechanism of forming the circulation is that the hot fluid is pumped from the heated surfaces and mixes with surrounding cold fluid especially that near the cold walls. The clockwise circulation has the negative sign and the anticlockwise circulation have positive sign. The number of circulation cells decreases when Ra increases as shown in Figure (3b) where it can be seen that cells in the upper two corners begin to fusion with the two strong cells localized in mid span of vertical walls. Due to the increase of convection effect here ($Ra=10^4$), it can be seen that the strength of circulation is higher than that of the above ($Ra=10^3$) approximately by a factor of 10. When Ra is further increases to 10^5, the circulation becomes stronger and more effective inside the enclosure as shown in Figure (3c) where the convection heat transfer is dominated over the conduction.

The isothermal lines for the same above parameters are gathered in the right side of Figure (3). According to the mechanism of fluid moving from around hot surfaces that previously mentioned, equivalent four plumes like distribution are jut out from the space between each two rods towards the enclosure center. This scenario is only observed at low Rayliegh number ($Ra=10^3$, Figure (3a) right. At high Ra ($Ra=10^4$), upper plum like diminishes, the two side plume like remain unchanged while the lower one is more arise towards the enclosure center. At higher Ra ($Ra=10^5$, Figure (3c) right), the lower plume

becomes more dominated in such a way it overcomes the other three plumes where the upper plum completely diminishes. This is an indication to the convection domination.

The effect of aspect ratio on the enclosure thermal performance is displayed in Figure (4) where the isotherms (right) and streamlines (left) are visualized for three aspect ratios (AR=0.16, 0.23 and 0.28) all for $Ra=10^4$. The effect of aspect ratio on the streamlines is shown in left side of Figure (4) where it can be seen that at lower aspect ratio (AR=0.16) the streamlines become more dense and an additional two cells are formed in the upper part of enclosure because of the available space which permits to fluid to freely circulate. Also it can be seen that the magnitude of stream function decreases with increasing the aspect ratio. This can be attributed to the lack in the space required to fluid circulation at higher AR. On the other hand, the isothermal lines (right side of Figure (4)) give more clarification to the above attribution where at higher aspect ratio the isothermal lines become more parallel and concentrated in the space between the rods and the outer wall of the enclosure.

5.2 Nusselt number

The distribution of local Nusselt numbers are examined along the circumference of inner rods and along the enclosure outer surfaces as follows: Figure (5) shows the variation of the local Nusselt number along the upper right rod for AR=0.23 and different Ra's. As can be seen from this figure, for $Ra=10^3$ at the upper point of the rod, the value of Nu_L increases with increasing of Ra and for $Ra=10^4$, the distribution of local Nusselt number Nu_L is similar where it reaches its minimum value at $S_1=0.375$ and increases sinusoidaly otherwise. At $Ra=10^5$, the distribution slightly differs, where along the segment $S_1=0.25$-0.5 we have larger values of Nu_L than that of low Ra and lesser otherwise. This is due to the plume like distribution of the isotherms through the space between the heated rods is greatly spread at high Ra due to the increase of the streamlines strength which dominates the convection. This scenario is clearly characterized from the isothermal lines of Figure (3). Where it is clear that the temperature gradient is minimum at $S_1=0.375$ for $Ra=10^3$ and $Ra=10^4$, and at $S_1=0.16$ for $Ra=10^5$. The Nusselt number Nu_L is proportional to temperature gradient; hence it will follow this variation in temperature gradient. The distribution of Nu_L along the lower right rod for the same parameters mentioned above is shown in Figure (6). The curves have a similar bell shape with one peak except at $Ra=10^5$ where two peaks are noticed. The values of Nu_L are increased with increasing Ra. For $Ra=10^4$, the Nu_L reduces from the top point $S_2=0$ to $S_2=0.375$ due to the domination of conduction heat transfer, then it increases gradually at the rod lower half part to make maximum values along the segment $S_2=0.5$-0.75. This may be

attributed to the enhancement of heat transfer process. For $Ra=10^5$, a similar trend is seen except it has two maximum peaks, one at the bottom point (S_2=0.5) and the other at the right point (S_2=0.75).

The minimum value of Nu_L appears at the point corresponding to the lower right corner of the enclosure (S_2=0.675). Figure(7) shows the Nu_L distribution along the outer boundaries of the enclosure for the same above parameter. For $Ra=10^3$ and 10^4, the distribution exhibits the same form, namely sinusoidal behavior with four M shaped peaks. Each peak is corresponding to one wall of the enclosure. Each zero value of Nu_L is corresponding to one corner. When Ra increases to 10^5, the behavior is completely differing from the lower Ra's. The vertical walls (left, S_o=0-0.25 and right, S_o=0.5-0.75) have the same behavior. The base (S_o=0.25-0.5) has a strong M shape and the lowest values of Nu_L due to the separation of isothermal lines between two lower rods and make a plume like distribution which in turn dominate the convection at the enclosure center and conduction near the bottom wall as can be seen from Figure3c right. The upper wall has sinusoidal distribution with very high values of Nu_L where it double times larger than other walls. This can be demonstrated by the steep temperature gradient along the upper wall of enclosure as in Figure(3c) right.

The effect of aspect ratio on Nu_L is studied by examine the variation of Nu_L for three values of AR=0.16, 0.23 and 0.28, with $Ra=10^4$. Figure (8) shows the variation of Nu_L along the upper right rod. A sinusoidal behavior is seen with all these aspect ratios. The interpretation of maximum and minimum regions of Nu_L is the same that discussed in Figure (5). But it can be seen from this figure that the values of Nu_L of AR=0.16 are higher than of AR=0.23 along all surfaces of the upper rod except that along the segment S_1=0.5-0.75 (where the value of Nu_L are approximately the same). This behavior is attributed to the following: at low aspect ratio, the surface area of the cylinder is reduced and these surfaces become farther from the cold outer walls of enclosure, hence the density of streamlines and flow strength here are higher as shown in Figure (4a) left when it compared with Figure (4b) left. From this figure also, it can be seen that the distribution of Nu_L for AR=0.28 has different localizations of maximum and minimum values. This due to that the hot surfaces become closer to each other and closer to the cold walls leading to high temperature gradients. Regarding with lower right rod Figure (9), we can say that the same reason above is the cause of alterations in the Nu_L values with aspect ratio, but the locality of this rod is the cause of the different localization of maximum and minimum values of Nu_L.

The effect of aspect ratio on Nu_L is greatly clarified in Figure (10) which shows the distribution of Nu_L along the outer walls of the enclosure. It appears from this figure how Nu_L

increases as AR increases. A general insight to this figure shows a repeated M shaped distribution along each flat wall of the enclosure. At the enclosure upper wall (S_o=0.75-1.0), the recorded Nu_L values are greater than otherwise especially at lowest aspect ratio. This may be attributed to that the moving up stream in low AR is dominated over that moving towards other walls. The M shape distribution is originated due to the reduction in temperature gradient between the walls (left, bottom, right and upper) and the space between the two neighboring rods i.e. the space of plume like origin as can be seen in isothermal lines of Figure (4) right.

Finally, the effect of the parameters under scope (Ra and AR) on the global heat transfer process is plotted in Figure (11) and Figure (12) respectively. It can be seen from these two figures that the mean Nusselt number is an increasing function of both Ra and AR. However it is well known that increasing Ra leads to a good mixing inside enclosure resulting in strong convection. On the other hand and as previously mentioned, increasing aspect ratio means two things, first; increasing the surface area of heating say element and second; nearness of the hot surfaces closer to the cold surface. Also it is worth mentioning to explain that at higher aspect ratio (large rods), and at higher Rayleigh number the wakes forming on the top of rods become larger i.e. separating of the fluid near the rod surfaces become earlier resulting in a good mixing which in turn increase the heat transfer.

6. Conclusions

The natural convection inside a square enclosure heated by four inner rods placed at equal distances from the enclosure center was studied numerically using a Galarkin finite element software package. The effects of aspect ratio (0.11-0.28) and Rayleigh number (10^3-10^5) on the heat transfer process were conducted. The following concluding remarks could be extracted from the obtained results:

1-As it expected and common reported in the literature, the stream function and the average Nusselt number are increasing functions to Rayleigh number.

2-The convection heat transfer could be enhanced by increasing the aspect ratio i.e. by increasing the surface area of the heated rods.

3- The effect of Rayleigh number on the mean Nusselt number is more significant at the lower aspect ratios.

4- Within the studied ranges of Rayleigh numbers and aspect ratios, the enhancement of mean Nusselt number due to the aspect ratio is more than that due to Rayleigh number.

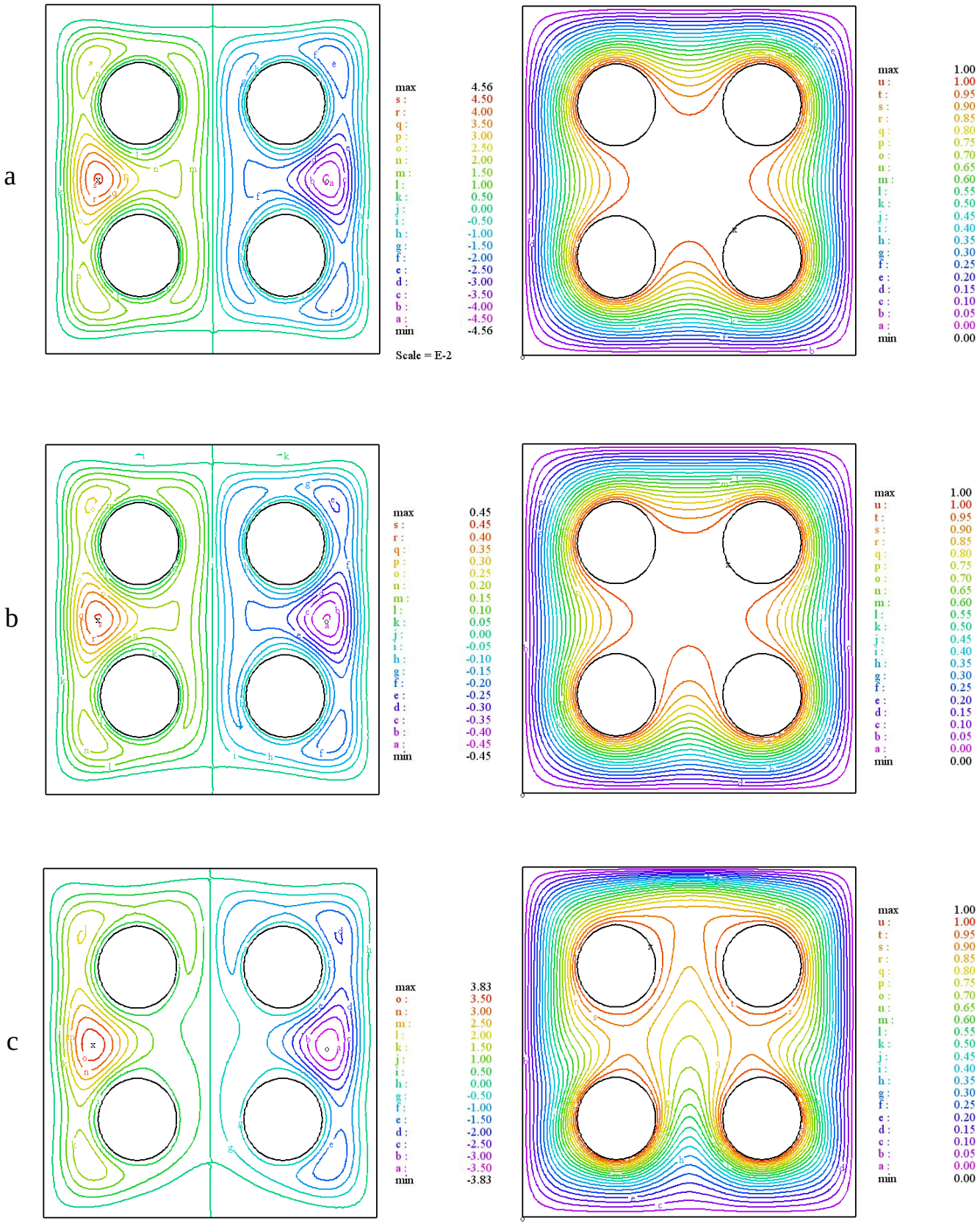

Figure(3). Streamlines (left) and isotherms (right) for AR=0.23, (a) Ra=10^3, (b) Ra=10^4, (c)Ra=10^5.

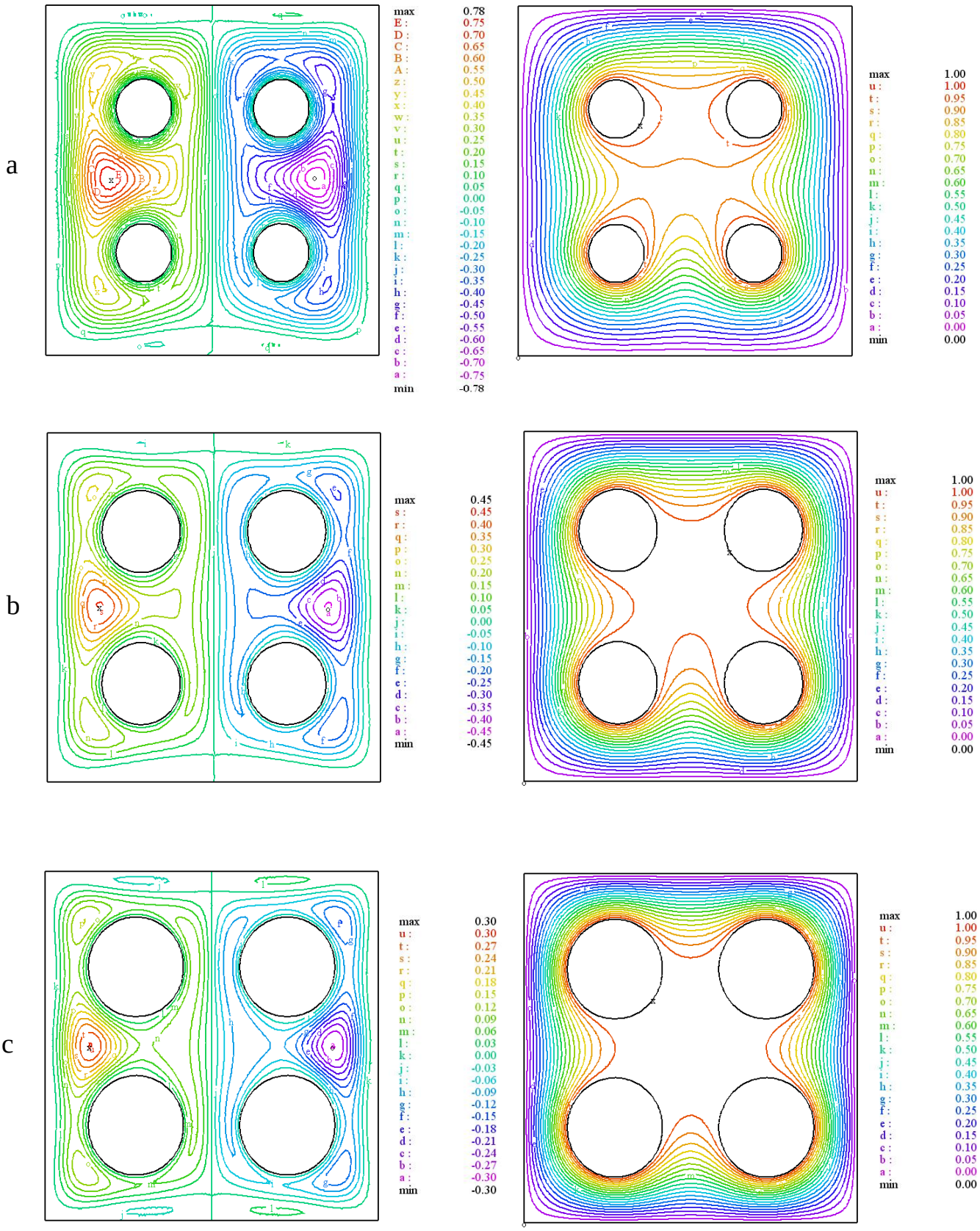

Figure (4). Streamlines (left) and isotherms (right) for $Ra=10^4$ (a) AR=0.16, (b) AR=0.23 (c) AR=0.28 .

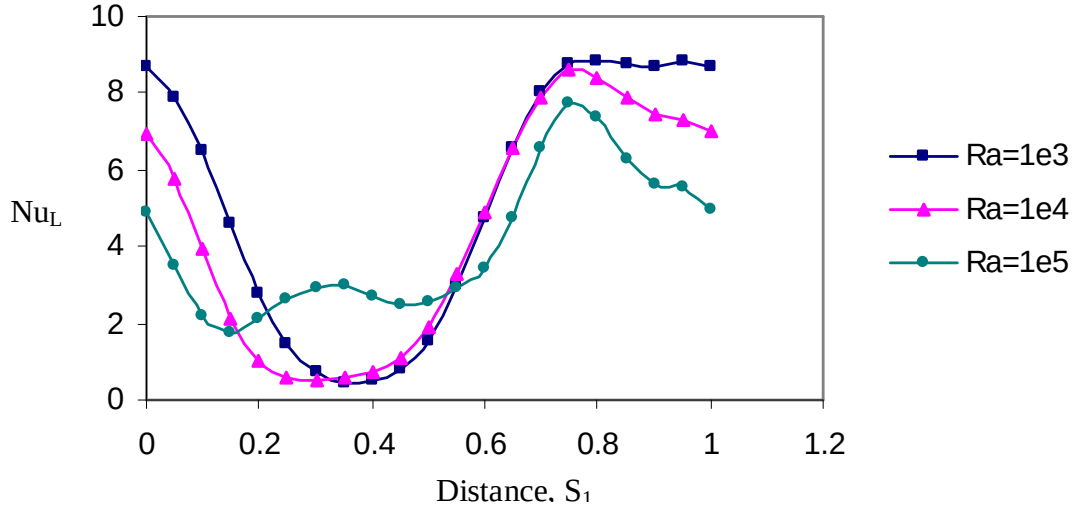

Figure (5). Variation of the local Nusselt number along the upper rod , AR=0.23 .

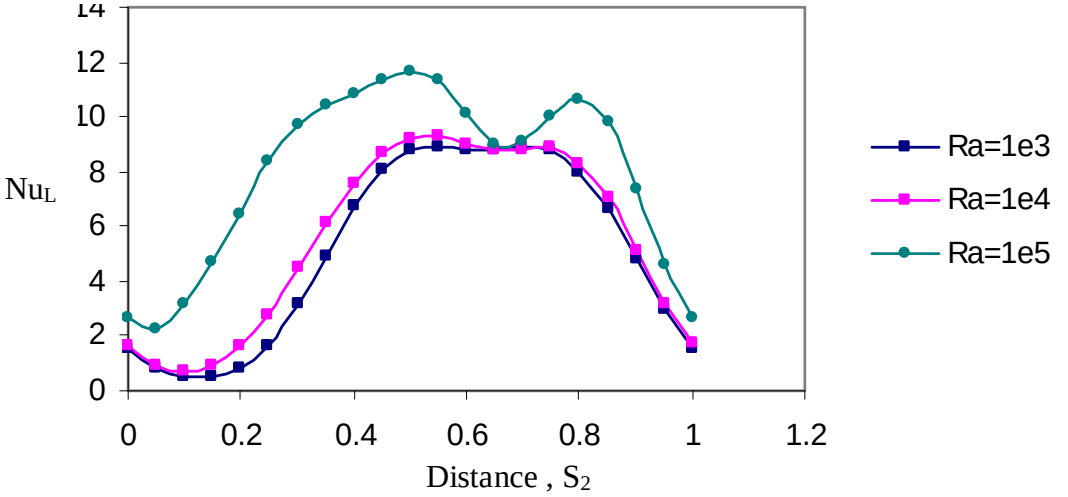

Figure (6). Variation of the local Nusselt number along the inner rod , AR=0.23 .

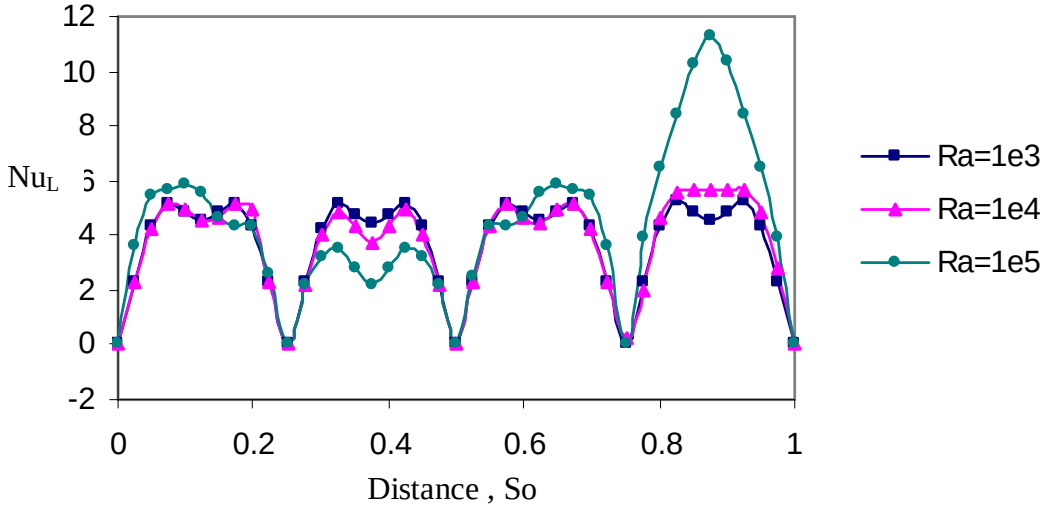

Figure (7). Variation of the local Nusselt number along the outer wall , AR=0.23 .

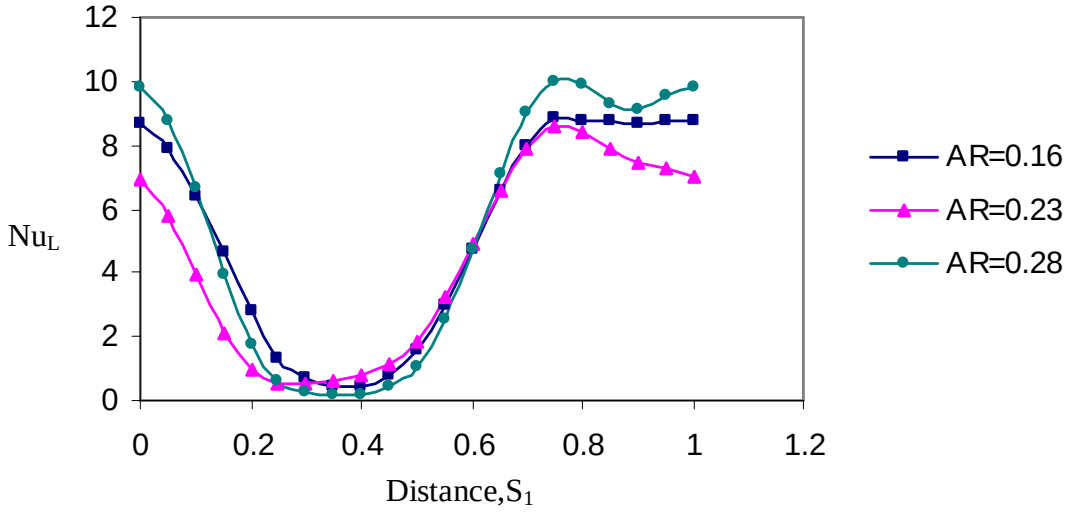

Figure (8). Variation of the local Nusselt number along the upper rod , Ra=10^4 .

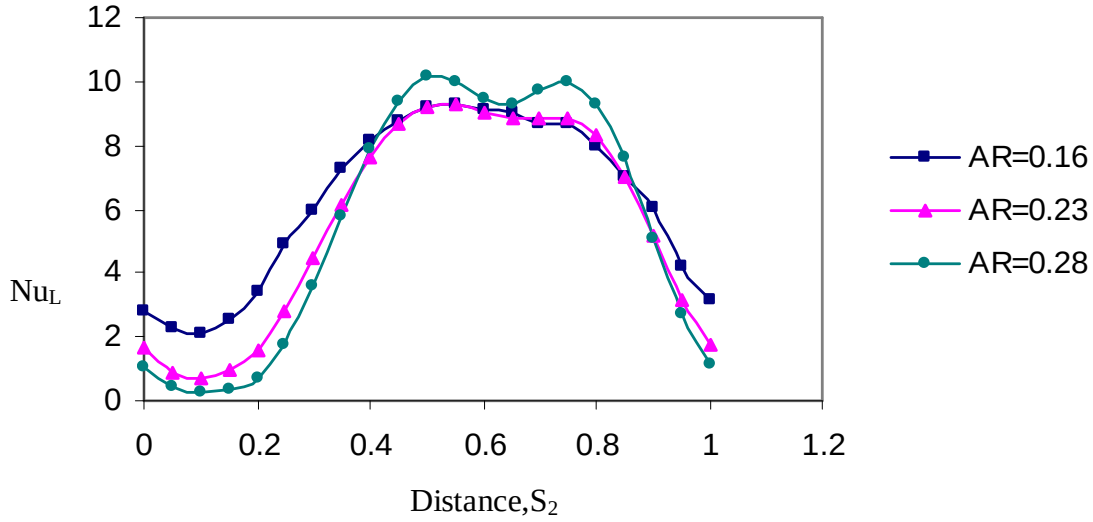

Figure (9). Variation of the local Nusselt number along the lower rod, Ra=$10^{4.}$

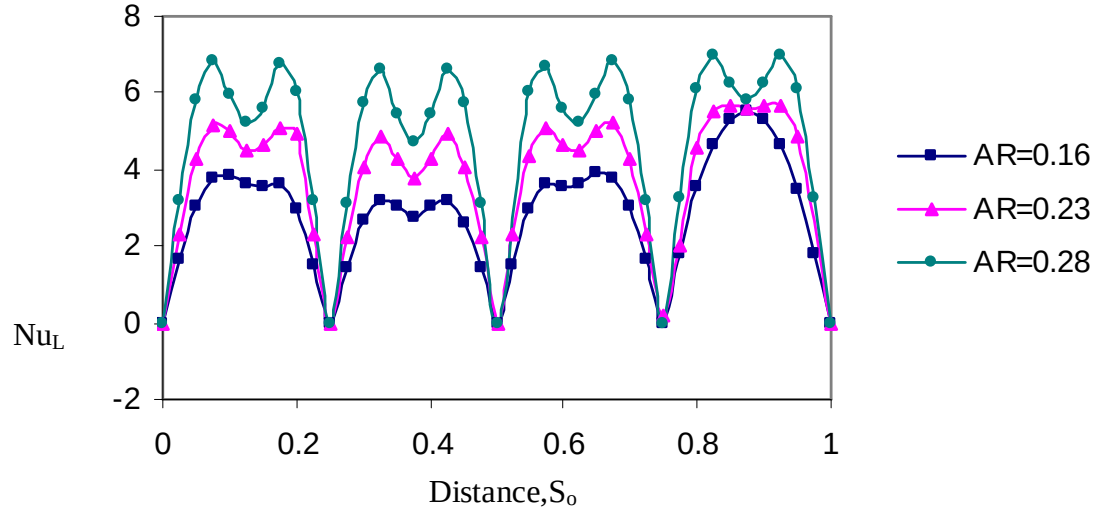

Figure (10). Variation of the local Nusselt number along the outer wall, Ra=10^4.

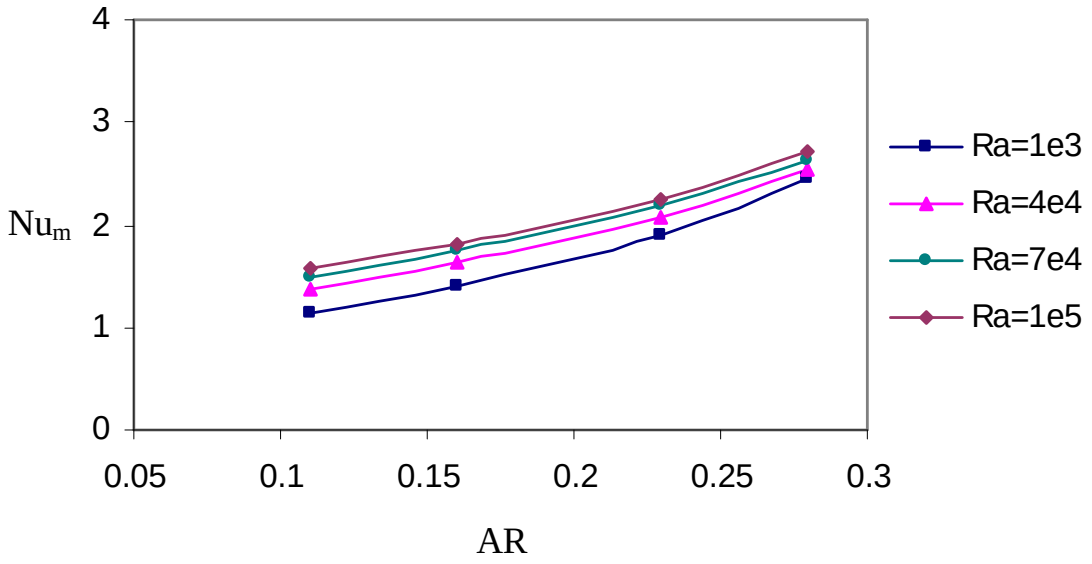

Figure (11). Variation of the mean nusselt number with aspect ratio along the outer wall for different Rayleigh numbers .

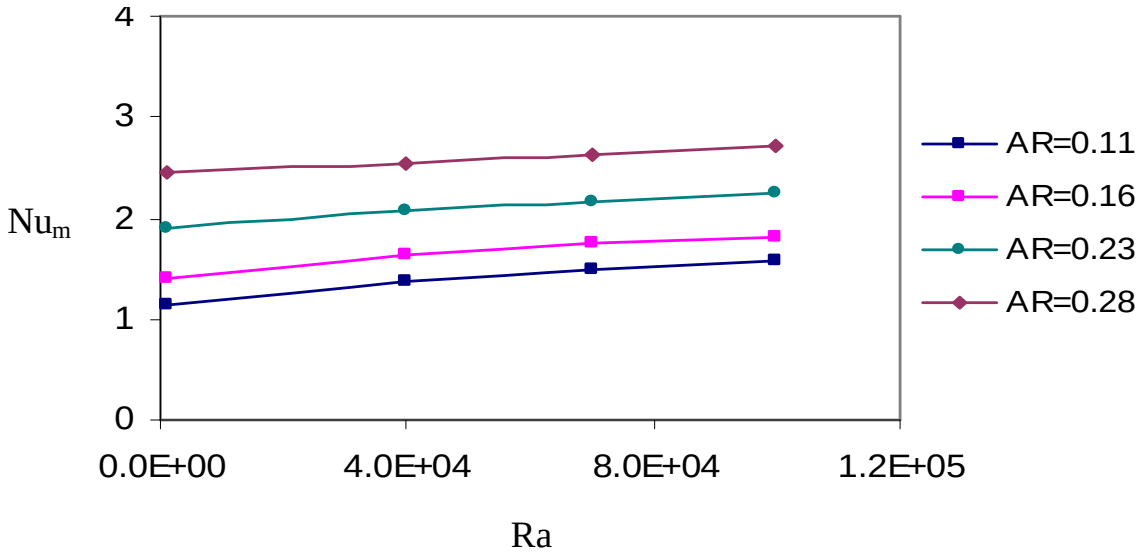

Figure (12). Variation of the mean nusselt number with Rayleigh number along the outer wall for different aspect ratios .

7. References

[1] Nicolette V.F., Yang K.T., Lioyd J.R., 1985, "Transient cooling by natural convection in a two dimensional square enclosure" Int.J.Heat Mass Transfer 28 1721-1732

[2] Hyun J.M., Lee J.W., 1989, "Numerical solution of transient natural convection in a square cavity with different side wall" Int.J. Heat fluid 10 146-151.

[3] Fusegi T., Hyun J.M., Kuwabare K., 1992, "Natural convection in a differentially heated square cavity with internal heat generation" Numer-Heat Transfer A21 215-229.

[4] Ganzarolli M.M., Malanez L.F., 1995 ,"Natural convection in rectangular enclosure heated from below and symmetrically cooled from the sides" Int.J. Heat Mass Transfer 38 1063-1073.

[5] Ekundayo C.O., Probert S.D. and Newborough M.,1998, "Heat transfer from a horizontal cylinder in a rectangular enclosure " APPL.Energy 61 57-78.

[6] Suh C., Xue H., Zhu Y.D ,2001, " Numerical study of natural convection in eccentric annulus between a square outer cylinder and a circular inner cylinder using DQ method" Int. J. Heat Mass Transfer 44 3321-3331.

[7] Shi X. J. Khodadi M., 2003, "Laminar natural convection heat transfer in a differentially heated square cavity due to thin film on the hot wall" J. Heat Trans 125 624-634.

[8] Saeid N.H., Yaacob Y. 2006, "Natural convection in a square cavity with special side-wall temperature variation" Numer-Heat Transfer. A49 (7) 683-697.

[9] Wu W., Ching C.Y. , 2008, "The effect of partitions on the laminar convection in square cavity" HT 2008-56193 in: 2008. ASME summer Heat Transfer conference. Jacksonville. Florida. USA 2008.

[10] Mobedi M., 2008, "Conjugate natural in a square cavity with finite thickness horizontal walls" Int. Conmum. Heat Transfer 35 503-513.

[11] Basak T., Roy S. ,2008, "Role of Bajans heatlines in heat flow visualization and optimal thermal mixing for differentially heated square enclosure " Int.J. Heat Mass Transfer 51 3486-3503.

[12] Wu W., Ching C.Y., 2009, "The effect of the top wall temperature on the laminar natural convection in rectangular cavities with different aspect ratios" J. Heat Transfer 131 1-11.

[13] Gunor Backstrom , 2005, "Field of physics by finite element analysis using FlexPDE" GB publishing and Gunner Backstrom Malmo, Sweedn.

[14] Roy S., Basak T., 2005, "Finite element analysis of natural convection flows in a square cavity with non uniformaly heated walls" Int.J.Eng.Sci 43 668-680.

[15] Moukalled F., Acharya S. ,1996, "Natural convection in the annulus between concentric horizontal circular and square cylinders " J. Thermophys. Heat Transfer 10(30)

8. Nomenclature

AR	aspect ratio D/L
Cp	specific heat (J/kg K)
D	diameter of circle (m)
g	gravitational acceleration (m/s^2)
h	heat transfer coefficient (W/m^2 K)
L	enclosure side length (m)
Nu	local Nusselt number
Nu_m	mean Nusselt number
p, P	dimensional and dimensionless pressure
Pr	Prandtl number
R	radius of circular rod (m)
RR	ratio of L/2R
Ra	Rayliegh number
s, S	dimensional and dimensionless local coordinates
T	temperature (K)
u, *U*	dimensional and dimensionless horizontal velocity component
v, *V*	dimensional and dimensionless vertical velocity component

Greek Symbols

Ψ	dimensionless stream function
θ	dimensionless temperature
α	thermal diffusivity (m^2/s)
β	thermal expansion coefficient (1/K)
ρ	fluid density (kg/m^3)
ν	kinematic viscosity (m^2/s)